Our J. O. 5044

Administered by

OFFICE OF NAVAL RESEARCH

Contract No. N8onr-60801
Project Designation No. NR-015-804

Supported by

Office of Naval Research
Bureau of Aeronautics
Atomic Energy Commission

TECHNICAL REPORT

Covering the Period January 1, 1953 to July 1, 1953

by

Robert O'B. Carpenter
Stanley J. Sage
Norman Hapgood

Submitted in accordance
with the terms of the
contract noted above.

Bruce Billings

Bruce H. Billings
Director of Research

Baird Associates, Inc.
33 University Road
Cambridge, Massachusetts

Table of Contents

ABSTRACT

The Fabry-Perot interferometer with mica cleavages as the spacer, as described in the last report, is completely investigated in this report. The properties of mica seem to render it impractical for the usage envisaged, namely, the variability from sample to sample in birefringence, the impossibility of cleaving to a prescribed thickness, and its absorption.

An ADP birefringent polarization filter, a unique type of tunable filter, is described and analyzed completely in this report. It is found that it is suitable for only moderate accuracy isotopic analysis. Part of its difficulty arises from the fine structure of $H\alpha$ and $D\alpha$, and this effect is analyzed. The other difficulties are the high tolerances required in flatness of plates and in temperature control.

I. Introduction

The work under this contract for the preceding nine months has been chiefly devoted to an investigation of tunable filter methods for isotopic analysis using atomic line spectro-chemical methods. For lines which have separations which are readily attained by the resolution of grating or prism spectrographs, standard spectrochemical techniques long in use in the metals industries and in other fields are directly adaptable, either using photographic plate-densitometer methods, or the more recent direct reading photomultiplier techniques.

There are two reasons why it might be of considerable scientific interest and technical importance to search for other dispersing means than a spectrograph. First, isotope shifts of spectral lines are in general very small, and only a very few are large enough to separate with any but the very largest grating spectrographs. The Fabry-Perot interferometer has long attained reputation and usefulness as the instrument par excellence for high resolution work. Secondly, even for a situation such as hydrogen-deuterium where the usual sized grating instrument is quite adequate in resolution, there is a possibility that much more compact, simple and inexpensive instruments can be designed by using some sort of interferometric technique to replace large grating spectrographs.

This contract in its inception some years ago was concerned with the development of tunable narrow band optical filters. Considerable experience has been had with both the standard Fabry-Perot interferometric techniques, and also with the less well known birefringent polarization interference filter.

It seemed natural to attempt to adapt some of these new optical techniques to the difficult and important problem of isotopic analysis.

Our last technical report, dated December 1, 1952, discussed the problem of hydrogen-deuterium analysis as an example of a general spectrochemical analysis problem in which there were only two lines whose intensity ratio was desired.

A particularly simple method for obtaining an accurate intensity ratio measuring instrument was described, by Mr. S. J. Sage, which in the following will be called the "Sage polarization method". This system consists of some variety of polarizing optical system, containing a rotating polarizer and an A.C. vacuum tube voltmeter null detector.

In that report a Fabry-Perot interferometer with a mica spacer layer used in conjunction with polarizers was suggested as one means of polarizing H and D light at right angles to each other so that the method could be applied.

During the past six months considerable experimental work has been performed looking toward the manufacture of the mica Fabry-Perot. Further, several other devices for producing the desired polarization effect in H-H light have been conceived, analyzed in some detail, and the experimental difficulties investigated. This report summarizes all that work which was done on this contract, in the period since the last report.

II. Elementary Theory of the Polarization H-D Analyzer

If a polarization device could be invented which presented these two spectrum lines, called H and D (after hydrogren and deuterium), in two states polarized at right angles to each other, then with a polarizer and a light detector or photocell, one could measure the intensities in each state of polarization and take the ratio.

Where there are considerable fluctuations in the light source, it might be desirable to spin a rotating polarizer which would then generate an A.C. signal in the photocell:

$$I = H \cos^2 \omega t + D \sin^2 \omega t$$

$$= \frac{H + D}{2} + \frac{H - D}{2} \cos 2\omega t \qquad (1)$$

Then if one could simultaneously measure the A.C. amplitude and the mean D.C. level, the relative intensities are easily obtained.

$$H \propto I_{DC} + I_{AC} \qquad (2)$$

$$D \propto I_{DC} - I_{AC} \qquad (3)$$

This first method requires a pair of accurate instruments to read the A.C. and D.C. amplitudes. A second method was conceived which requires a polarizer mounted on an accurately calibrated circle, with the only electronic equipment needed being an A.C. null detector. This general method was described in detail in the last report, and extensive experimental tests were described which were aimed at determining the limits of accuracy of such a method.

Briefly, in all the modifications of this method, the inten-

sity of the light incident on the photocell is made to follow the relation

$$I = D \cos^2 \theta \cos^2 \omega t + H \sin^2 \theta \sin^2 \omega t \qquad (4)$$

(equation (1) of the last report), where H and D are the intensities of the two light beams to be analyzer, θ is the angle of the calibrated polarizer and ωt is the angle of the rotating polarizer.

If now the calibrated polarizer is turned to such an angle that

$$D \cos^2 \theta_o = H \sin^2 \theta_o \qquad (5)$$

then, because $\cos^2 \omega t + \sin^2 \omega t = 1$, the photocell current has no A.C. component, and a null balance is obtained. The angle θ_o is read from the calibrated circle and the intensity ratio is immediately found from

$$D/H = \tan^2 \theta_o \qquad (6)$$

The accuracy of the method is limited by the accuracy with which the calibrated circle can be set and read, and by the accuracy with which the null detector can locate the balance. If $\Delta \theta_o$ is the error in setting or reading the circle due to some optical or mechanical difficulty, and ΔI_{AC} is the minimum detectible departure from balance which the null detector can observe (or the noise level from some electronic source), the corresponding relative errors in the D/H deterimination are

$$\frac{\Delta (D/H)}{D/H} = \frac{1}{\tan^2 \theta_o} \frac{d}{d \theta_o} (\tan^2 \theta_o) \Delta \theta_o$$

$$= 4 (\csc 2\theta_o) \Delta \theta_o \qquad (7)$$

and

$$\frac{\Delta D/H}{D/H} = \frac{4 (\csc 2\theta_o)}{(d I_{AC}/d\theta)_{\theta_o}} \Delta I_{AC} \qquad (8)$$

III. Rotation of Quartz

The rotation of the plane of polarization by z-cut crystalline quartz immediately suggests itself as the most straightforward means of producing the differential rotation of the H and D lines for analysis by the Sage method. A study of the numerical properties of quartz in this application, however, shows that the path length is quite impractical.

The specific rotation of quartz at H_α is listed by the Chemical Rubber Company "Handbook of Physics" as 17.318 degrees per millimeter. With varying wavelength the rotation R of quartz follows an equation of the type

$$R = K/\lambda^2 \tag{9}$$

where K is a constant. Therefore for a small separation between two lines, $\Delta\lambda$, the change in rotation is

$$\Delta R = 2\,\frac{K}{\lambda_o^3}\,\Delta\lambda = -2\,R_o\,\frac{\Delta\lambda}{\lambda_o} \tag{10}$$

For the desired application we must have $\Delta R = 90$ degrees. For $H_\alpha - D_\alpha$,

$$\frac{\Delta\lambda}{\lambda_o} = \frac{1}{3680} \tag{11}$$

so that we require a quartz plate of rotation $90 \times 1840 = 165{,}600$ degrees. This is 9.55 meters of quartz. Since the supply of quartz is already dangerously scarce, it was thought best to discontinue consideration of this possibility.

IV. Experiments with the Mica Fabry-Perot Interferometer

The excellent results reported previously on the accuracy of the Sage null detector for determining the ratio of two light beams polarized at right angles were very encouraging, so experiments were undertaken to develop an isotope comparator based on this method. The comparative simplicity of the spectra of hydrogen and deuterium, availability of some samples and sources, and the general usefulness of H-D analysis were controlling reasons for choosing this pair of isotopes for the first practical experiments.

The Fabry-Perot interferometer with spacer layer of mica, as previously discussed, seemed to be one of the simplest possible devices for producing the light polarization. Mica is a birefringent material which cleaves readily and thus avoids the problem of laborious and expensive polishing of optical surfaces. Cleavage plates of mica were then coated in an evaporator with both silver and multilayer dielectric reflective layers on both sides. The silvered plates were not usable, for when the absorption of the silver layers was added to the natural absorption in the mica, the peak transmission in theFabry-Perot fringes was inadequate. The multilayer technique proved more successful, in this regard, as layers of high reflectivity with almost no absorption can be made by this method.

Since mica is a birefringent material, when it is used as the spacer layer in a Fabry-Perot interferometer, there will be two independent sets of approximately circular fringes, one for each refractive index. These are polarized at right angles to each other. They have been discussed by Pfund[1] and by Billings[2].

1. A. H. Pfund, J. Opt. Soc. Am., 32, 383 (1942)

2. B. H. Billings, J. Opt. Soc. Am., 34, 267 (1944)

The two fringe sets do not have exactly the same contours, and there are places in the angular field of the crystal where the peaks coincide and other places where they are out of step. With light of two wavelengths incident, such as H and D. there are then four sets of fringes. One would like to choose thickness, birefringence, or the angle of viewing so that at the point in the angular field selected by the slit of the optical system the H peak of one index fringe coincides with the D peak of the other index fringe. By taking wide angle photographs through the mica Fabry-Perot with a polarizer, first along one crystal axis, then along the other, then without polarizer, it is relatively easy to determine where this superposition of fringes occurs.

During the course of experiments with both silver and multilayered mica plates some 20 plates were made. Figure 1 shows six typical plates. The top three have multilayer reflective coatings, and the bottom three have silver. Of these one was found to be considerably better than the others, and most of the photographs were taken with this one. In Figure 2 is sketched the layout of equipment for taking these photographs. Figure 3 shows some of the typical photographs taken. No polarizers were used, so both sets of fringes are shown. The two strong fringes of H-alpha come from the ordinary and extraordinary rays. The weaker D-alpha fringes can be observed in the lamps containing D_2, and there are places where the ordinary H fringe coincides with the extraordinary D fringe. Figure 4 is a photograph of the equipment sketched in Figure 2.

The difficulties in taking such plates were very great because of the random characteristics of the two refractive indices of mica. Each mica plate examined showed a different set of refractive index values. In addition, for any given mica plate, although the proper thickness might be computed, it was impossible to obtain this thickness since the cleavage of mica is again a random process. A laborious procedure of constructing

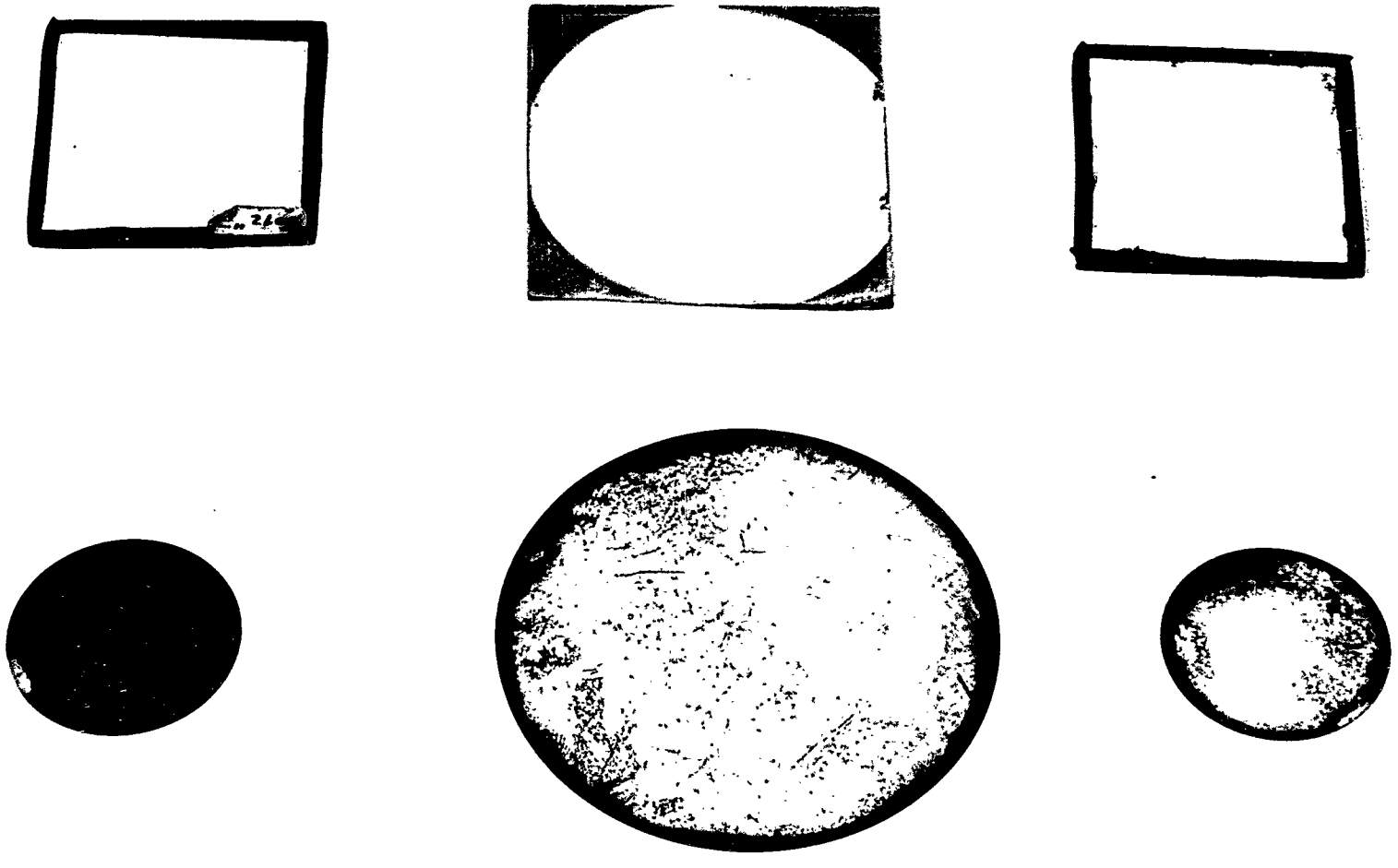

FIGURE 1. MICA FABRY-PEROT PLATES.

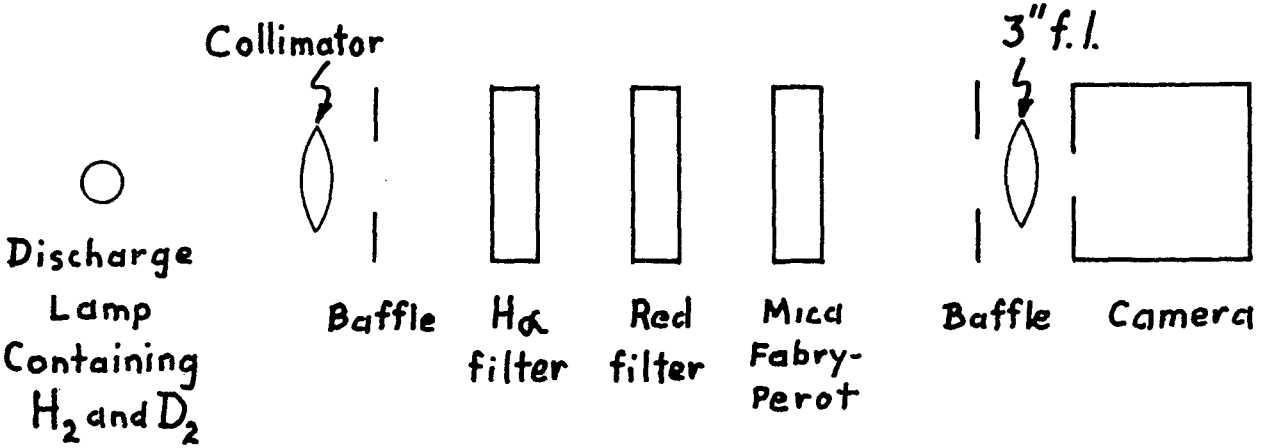

Fig. 2

Arrangement for Photographing Mica Fabry-Perot

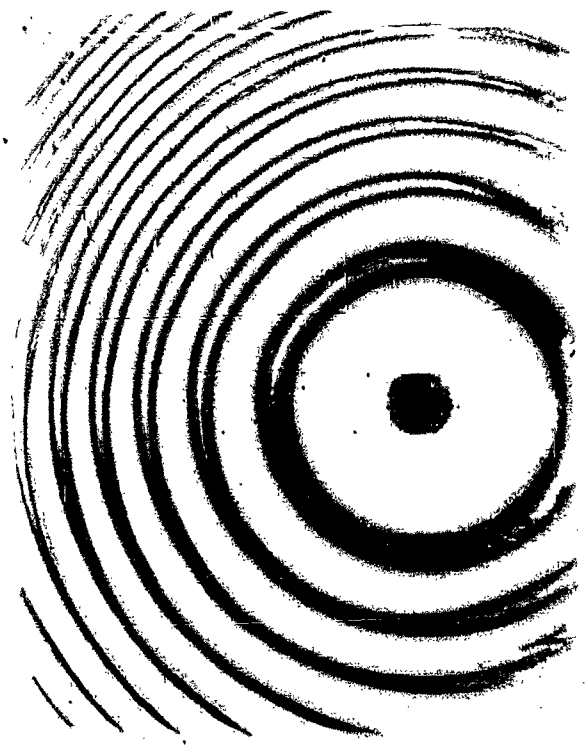

NATURAL H_2 LAMP

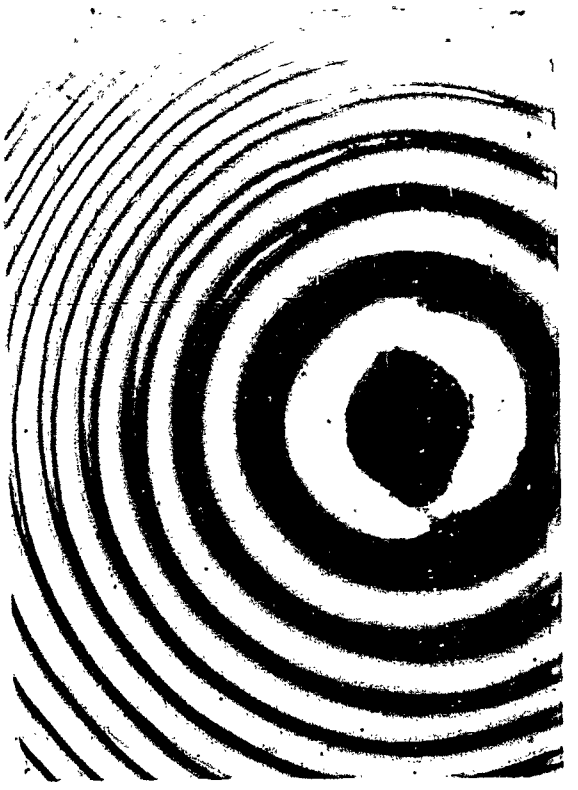

ABOUT 95% H_2 , 5% D_2 .

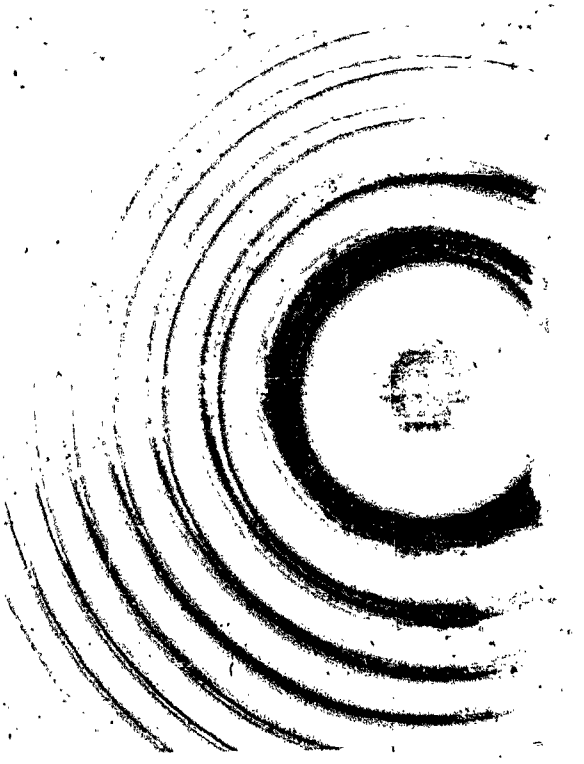

ABOUT 70% H_2 , 30% D_2 .

FIGURE 3. FABRY-PEROT INTERFERENCE FRINGES FROM MICA COATED WITH MULTILAYER REFLECTORS.

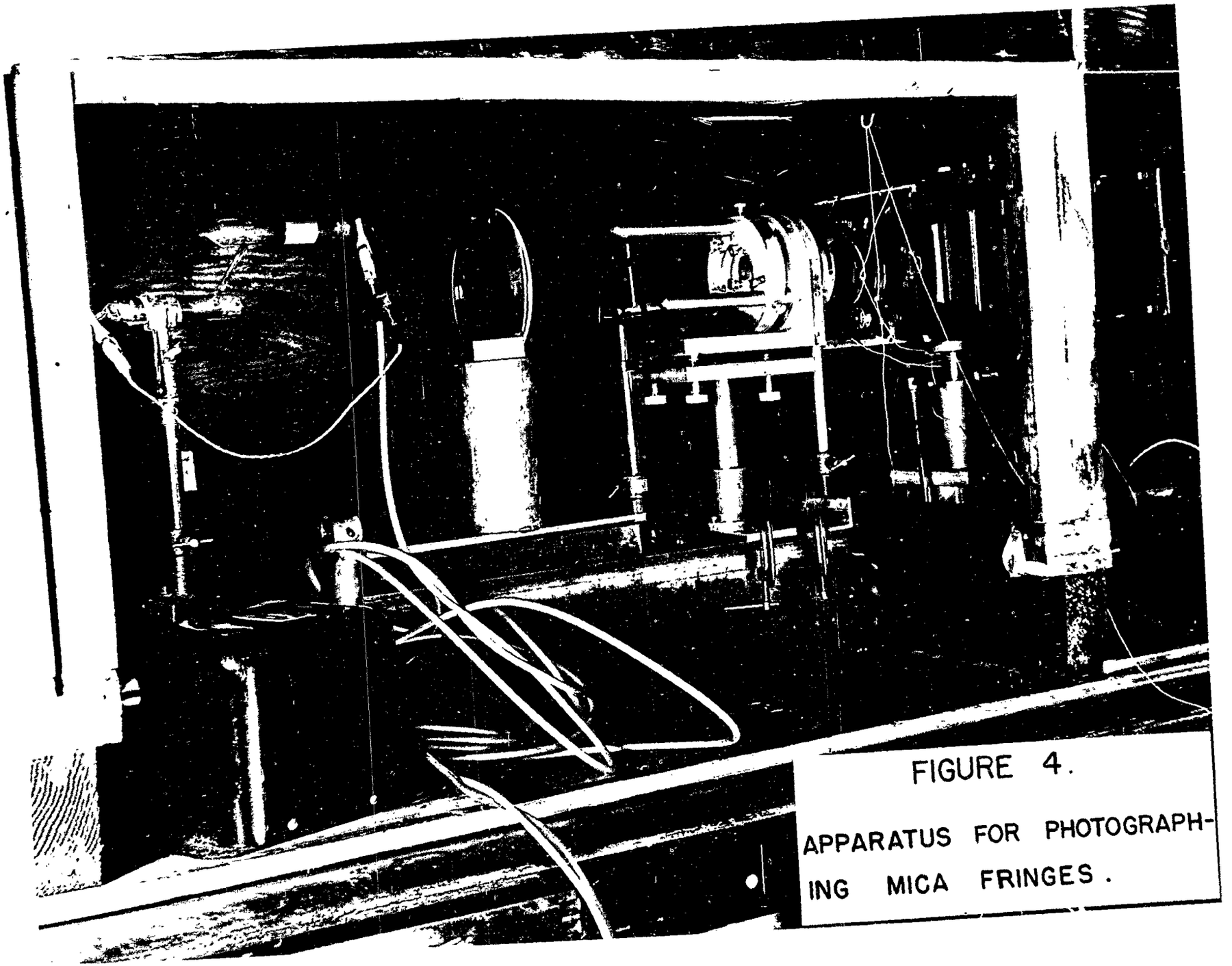

FIGURE 4.

APPARATUS FOR PHOTOGRAPHING MICA FRINGES.

and examining mica interferometers made from random samples was undertaken to determine the frequency of suitable samples in the necessarily random group that must be used. After examination of some twenty samples only one with any possibility of usefulness was found, and even for this one, the complete separation of the radiation from the two isotopes could not be obtained.

In addition to the difficulty of predicting the birefringence or the thickness of a cleaved mica plate, mica suffers from absorption of light throughout the visible. The color or absorption versus wavelength of mica varies considerably from sample to sample. In a Fabry-Perot interferometer absorption in the spacer layer is a much more discouraging phenomenon than absorption in the reflection layer. Absorption in the reflection layer only decreases the overall transmission of the interferometer without affecting at all the fringe sharpness and shape. Absorption in the spacer layer, on the other hand, reduces the "visibility" or contrast of the fringes, hence the resolution. It was for this reason that even the sample with perfect superposition of fringe peaks was unable to obtain sufficient discrimination from the other wavelengths lying one-half fringe order away. The subject of the contrast of the Fabry-Perot will be treated in more detail later when we return to interferometers with air and quartz spacers, which are quite transparent.

V. Experiments with Birefringent ADP Plates

The results of the mica investigation made it apparent that new technique would be required to resolve H and D in a polarization apparatus with sufficient discrimination to make a useful analyzer.

Past experience at Baird Associates, Inc. has demonstrated that polarization interference plates can be constructed of ADP to tolerances of five millionths inch or better. An analysis was undertaken to determine whether a suitable polarization interferferometer might be constructed using these plates.

ADP is a purely birefringent uniaxial crystal, that is, it has no circular birefringence, does not rotate the plane of polarization. However, there is a theorem in polarization optics, most explicitly stated by Jones,[3] that an effective optical rotator can be constructed from a combination of birefringent retardation plates. The mathematics for treating combinations of retardation plates can be handled in numerous ways, involves mostly trigonometric identities. One of the most convenient standardized procedures is to use the "generalized intensity formulas" of Hsu, Richartz, and Liang[4] for the intensity transmitted by combinations of retardation plates between polarizers. After considering a number of systems based on this general principle, the following system evolved as the one most simply constructed.

3. R. Clark Jones, J. Opt. Soc. Am., 31, 500 (1941).

4. J. Opt. Soc. Am., 37, 99 (1947).

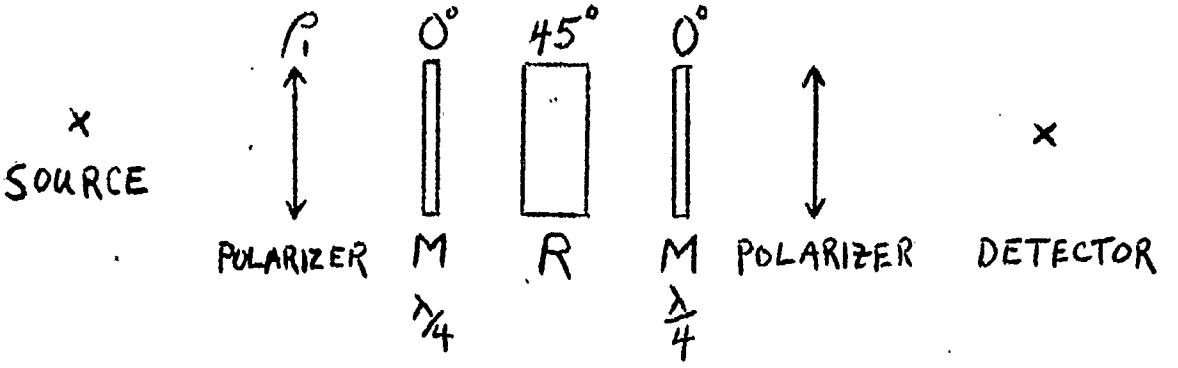

M is a quarter-wave retardation plate of mica. R is a thick retardation plate for which ADP, calcite and quartz will eventually be considered. The angles written at the top are the azimuths of the polarizers and wave plates measured from some convenient reference azimuth. By means of the Hsu, et al, method it can readily be shown that the transmission of such a system is given by

$$T = \cos^2(\gamma + P_1 - P_2) \qquad (12)$$

where γ is one-half the phase retardation of the thick plate R. If n is the thickness in waves, $\gamma = \pi n$. Now it is necessary to choose the thickness of R such that

$$\gamma_D - \gamma_H = \frac{\pi}{2} = 90^\circ \qquad (13)$$

for then the system has the same transmission as the rotatory quartz system discussed previously. This is what is meant by the "rotation equivalence" theorem. For equation (12) is also the equation for the transmission of a rotator of angle γ between polarizers at angles $P_1 + P_2$.

The experiments were performed with a system representing essentially two of the above systems in series. This is done in order to make use of the calibrated polarizer-null balance method. With two "equivalence rotators" in series, the first system rotates the H and D light until it is orthogonal. The middle polarizer is oriented somewhere between these two orthogonal directions of polarization of H and D at an angle which attenuates the stronger components till it matches the

weaker. The final polarizer scans between H and D at the rotation frequency of the rotor. The final system as thus derived looks like the following. An additional refinement has been added in the form of an angular field widening system[5] in which the thick plate R is cut in half, the two halves rotated by 90 degrees and a half-wave plate inserted between them.

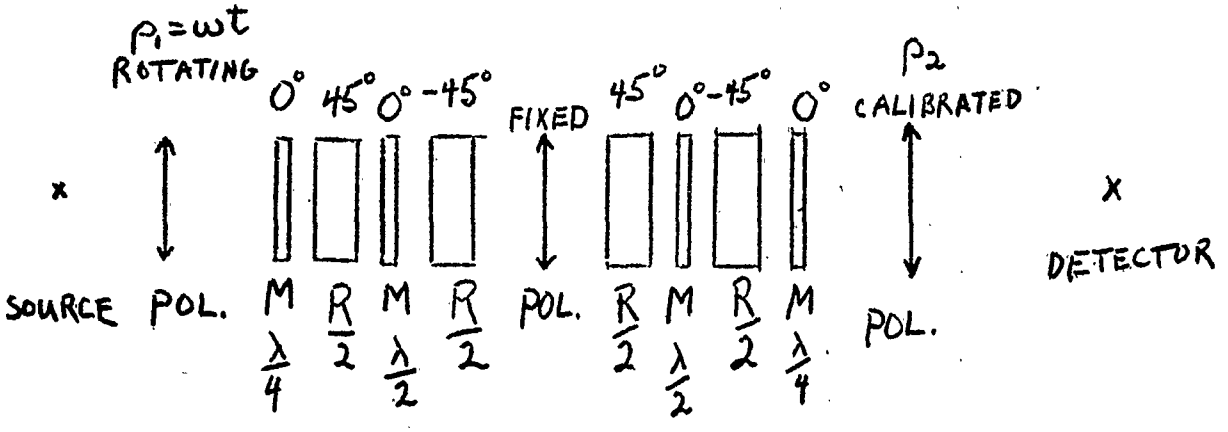

Figure 5

The transmission of this system is given by

$$T = \cos^2(\gamma - \rho_1)\cos^2(\gamma - \rho_2) \qquad (14)$$

This system requires four identical thick retardation plates R/2. The condition (13) determines the necessary thickness of birefringent crystal from the polarization interference equation

$$\gamma = \frac{\pi \mu t}{\lambda} \qquad (15)$$

where μ is the birefringence, λ the wavelength, and t the thickness of the crystal plate.

5. Described by Evans, J. Opt. Soc. Am., 39, 229 (1949)

$$\frac{\Delta\delta}{\delta_o} = -\frac{\Delta\lambda}{\lambda_o} \qquad (16)$$

If $\Delta\delta$ is to be $\pi/2$, $\delta_o = 3680\pi$, $n = 1840$ waves. Since $\mu = .0446$, the thickness t for ADP is about 2.71 in. Four identical plates of half this thickness are required for the field widened system.

A number of such plates were available at Baird Associates, Inc. in connection with the work on the solar $H\alpha$ polarization interference filter. These are listed in stock according to waves retardation at $H\alpha$. By superposing a few of the stock thickness it was possible to obtain plates sufficiently close to the required value of 920 waves.

The initial experiments consisted of setting up the polarization filter as described above in a collimated light beam. The source was an H-tube type Geissler discharge containing both H and D gases. A red glass filter was suitable to isolate the $H\alpha$ and $D\alpha$ lines at the entrance to the polarization apparatus. The output was picked up by a photomultiplier tube and displated on a cathode ray oscilloscope. The spinning polarizer was rotated at 60 cps. It was very difficult to obtain any satisfactory results from this arrangement since the 120 cycle rectified output of Geissler discharge caused sufficient noise in the output to obscure the signal. A source change was made to a 2450 Mcps microwave exciter and an electrodeless lamp containing both H and D.

Experiments using this source demonstrated that it too contained 120 cycle modulation which some simple additional filtering of the magnetron power supply was unable to eliminate. An attempt was made to use a General Radio narrow band tuned amplifier and a variable speed motor on the rotating polarizer to eliminate the source modulation effect, but since an A.C. null was to be the criterion of match, even the low resultant source modulation was found to destroy the sensitivity. Further experimentation into the construction of a regulated D.C. operated source was undertaken

and the interferometer was in the meantime modified to permit visual observation so that source modulations would have no effect. For this purpose the rotating polarizer was replaced by a split field analyzer (two polaroids mounted at exactly 90 degrees to each other and each covering about half the field). By this technique the extreme values of the intensity observed by the rotating polarizer could be compared, and the A.C. null setting would be replaced by a matched field setting.

This matched field setting is obtained by rotating P_2 from the position of maximum field difference through an angle θ_2 to minimum field difference, i.e., matched fields. The relative concentrations for H, D are simply formed for the ideal case by the relationship

$$\frac{C_D}{C_H} = \tan\theta \text{ whence } \begin{matrix} C_D = \sin^2\theta \\ C_H = \cos^2\theta \end{matrix} \qquad (17)$$

Since the settings are determined by comparing the two fields of the split polarizer, it was considered important the axes of the split polarizer be exactly 90° apart. After extremely careful cutting and mounting polarizing sheet (Polaroid HN36), a split polarizer was built with axes rotated by 89.3°. Since no closer accuracy could be obtained, the polarizer was used in the following experiments since further analysis mathematically shoed that no variation in θ might be expected from this deviation.

$$I_1 = I_H \sin^2\theta_2$$

$$I_2 = I_D \cos^2\Delta \cos\theta_2 + I_H \sin^2\Delta \sin\theta_2 \qquad (18)$$

where I_1, I_2 are the intensities observed in the two halves of the field. The maximum difference occurs for $\theta_2 = 0$, the matched field occurs for

$$I_H \sin^2\theta_2 (1-\sin^2\Delta) - I_\Delta \cos^2\theta_2 \cos^2\Delta = 0 \qquad (19)$$

For this case, it is obvious that while the sensitivity may be slightly varied, the value of θ_2 that satisfies this condition is independent of Δ, the deviation from orthogonality between the split field polarizer axes.

For these experiments the interferometer was set up as before except that the spinning polarizer was replaced by the split field polarizer and the photo tube by an eyepiece.

There ensued a period of experimentation which was composed almost completely of attempts to remove the variations from the ideal case which must be encountered in practice. The problems encountered included variations in retardation because of the high sensitivity of ADP to temperature, small variations of the retardation plates in azimuth or incident angle which reduced the effectiveness of the assembly. Angular field limitations proved extremely troublesome as well as multiple reflections between elements.

Each of these problems necessarily caused an increase in sophisticated apparatus to solve it. The reflection and temperature change were reduced by immersing the unit in a temperature controlled oil bath. The angular field limitation problem was resolved by using, instead of a single thick ADP plate of retardation η, two plates each having a retardation $\eta/2$. These plates, when adjusted as in Figure 5, will have a retardation η and an angular field about eight times greater than the single ADP plate.

Despite all these precautions the sensitivity obtained was still rather poor, primarily because it was impossible to produce complete extinction in either field at any time.

The lack of extinction could have been caused by one of two effects. First, poor extinction might be caused by small variations in retardation due to small temperature or thickness variation effects, or secondly, it might be because each isotope produced not pure monochromatic radiation, but rather a fine structure spectrum which could be resolved into two lines with about 1/15 the separation between the Hα and Dα.

To ascertain accurately which of these conditions applied, it was decided to examine each separately. Therefore, the source was changed to a discharge lamp containing only Hg198, an isotope having extremely monochromatic radiation at 5461 Å.

The entire apparatus was rebuilt to permit the use of this wavelength, and after extensive and careful experimentation it was determined that the extinction qualities of the interferometer using this wavelength were better but still far from ideal.

A simple analysis showed that the presence of two wavelengths for each isotope might have an extensive effect on sensitivity for low concentrations.

This effect seemed large enough so that a complete mathematical analysis of the sensitivity variations as a function of multiple wavelengths, temperature and thickness variation was undertaken.

Figures 6 to 10 show photographs of the apparatus as finally assembled in conjunction with its oil bath. Figure 6 shows a view of the front end of the oil bath. Figure 7 shows the calibrated polarizer and eyepiece for visual viewing during alignment of the plates. Figure 8 shows the rotating polarizer, lens and mount for the 1P22 photomultiplier detector. Figure 9 shows the calibrated polarizers and some of the set of ADP and mica plates used in assembling the system. Figure 10 shows some

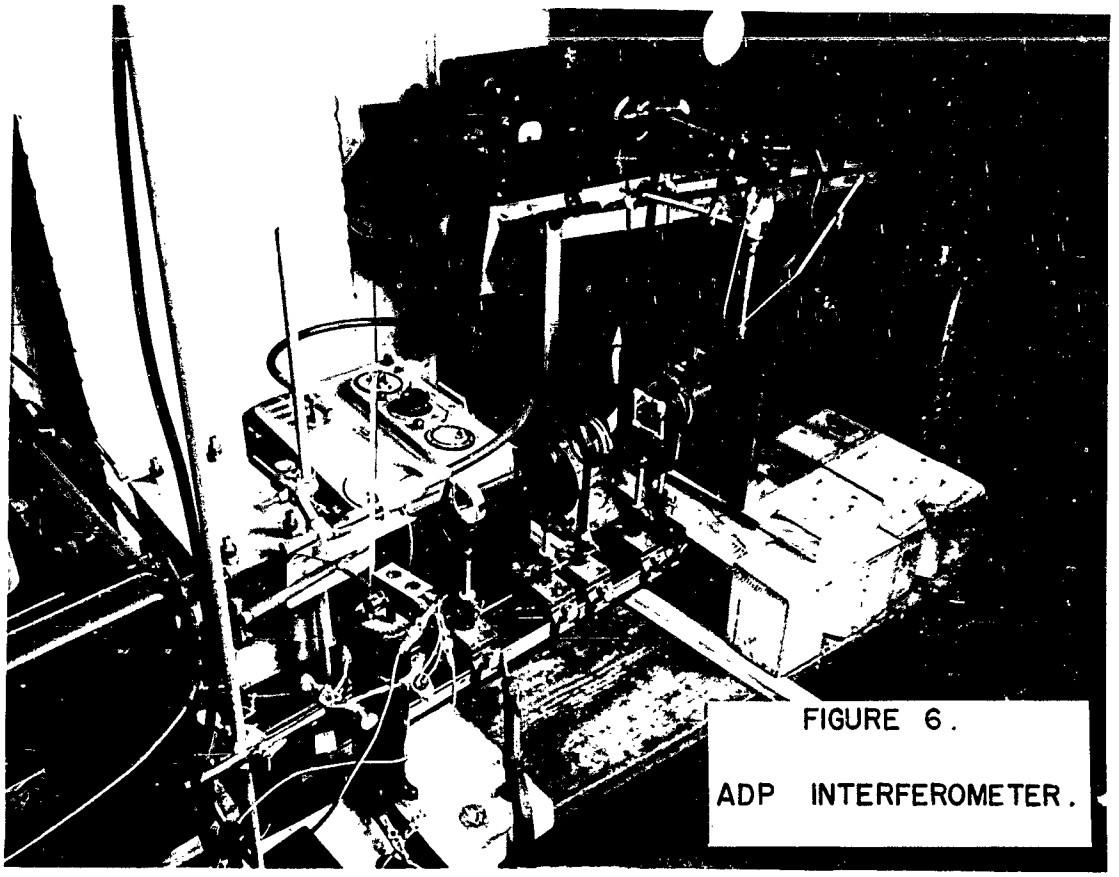

FIGURE 6.

ADP INTERFEROMETER.

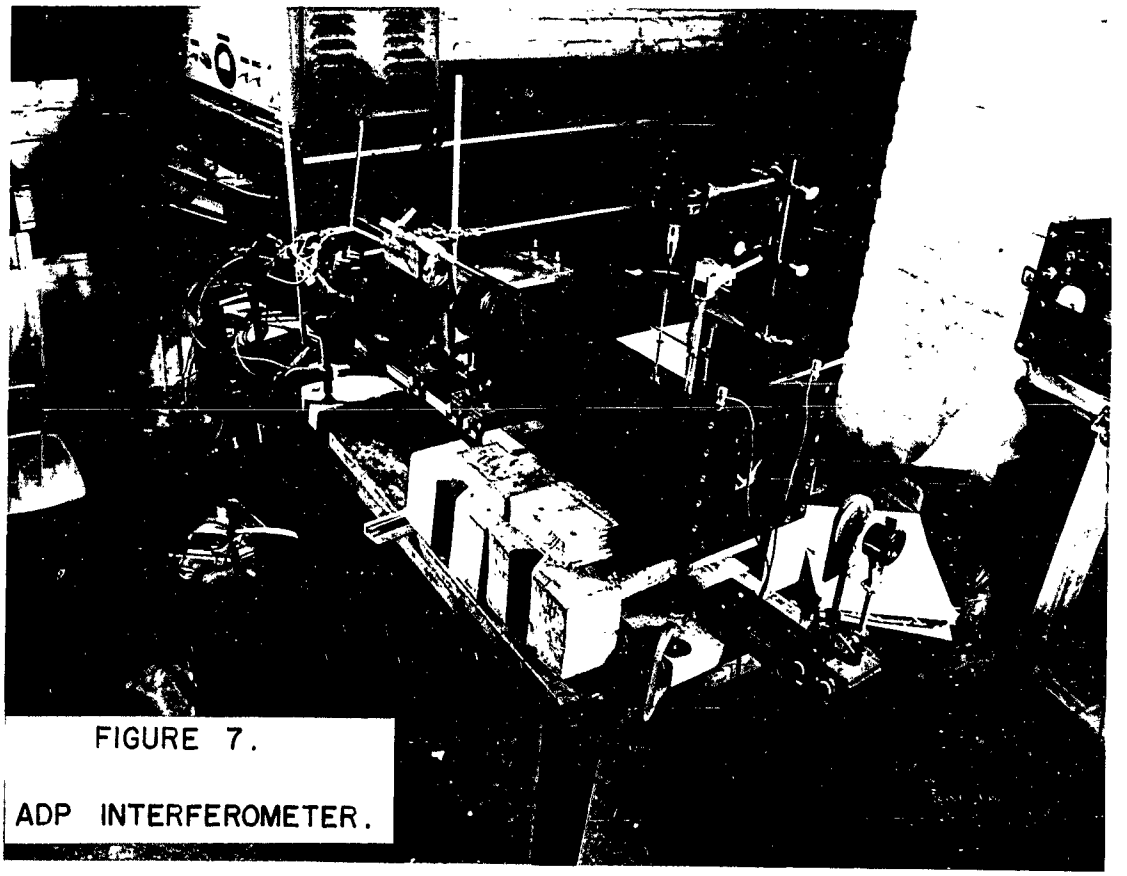

FIGURE 7.

ADP INTERFEROMETER.

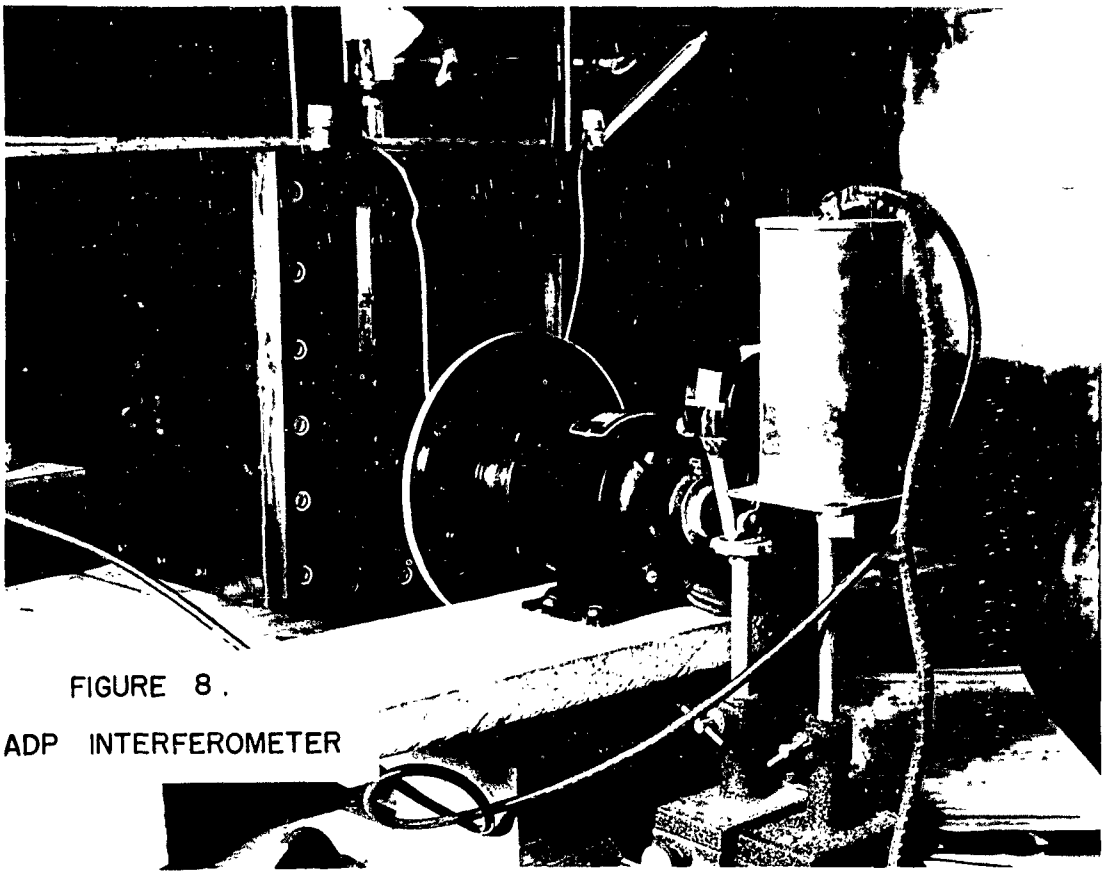

FIGURE 8.

ADP INTERFEROMETER

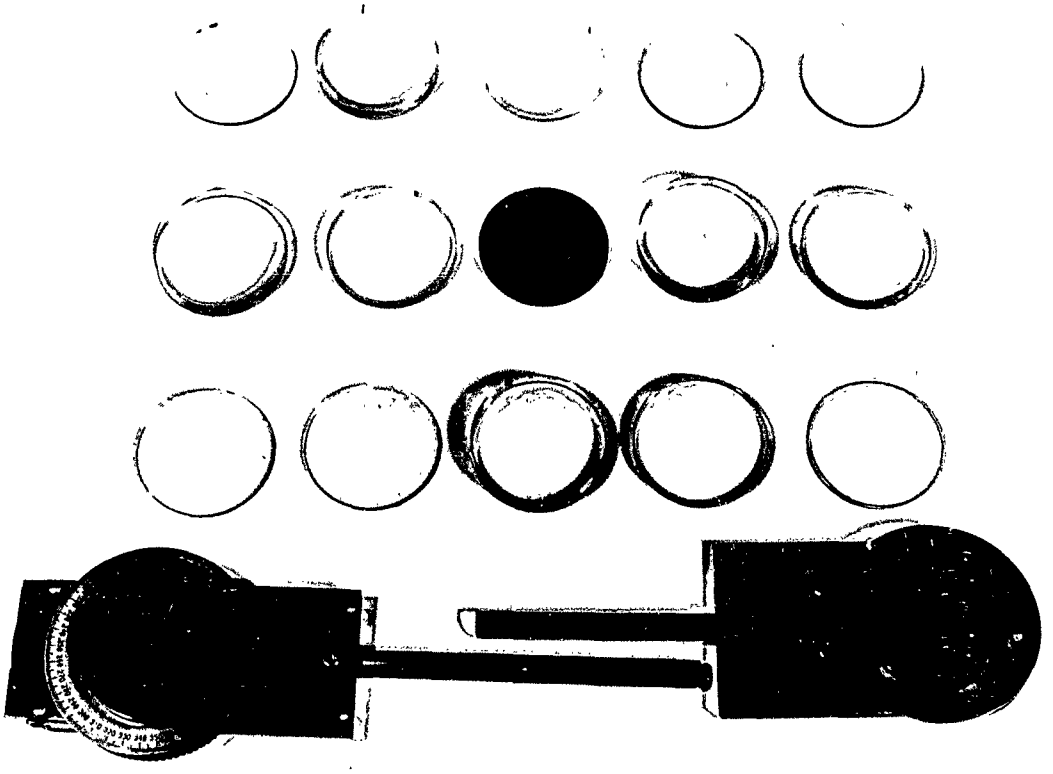

FIGURE 9. ADP. MICA PLATES AND CALIBRATED POLARIZERS.

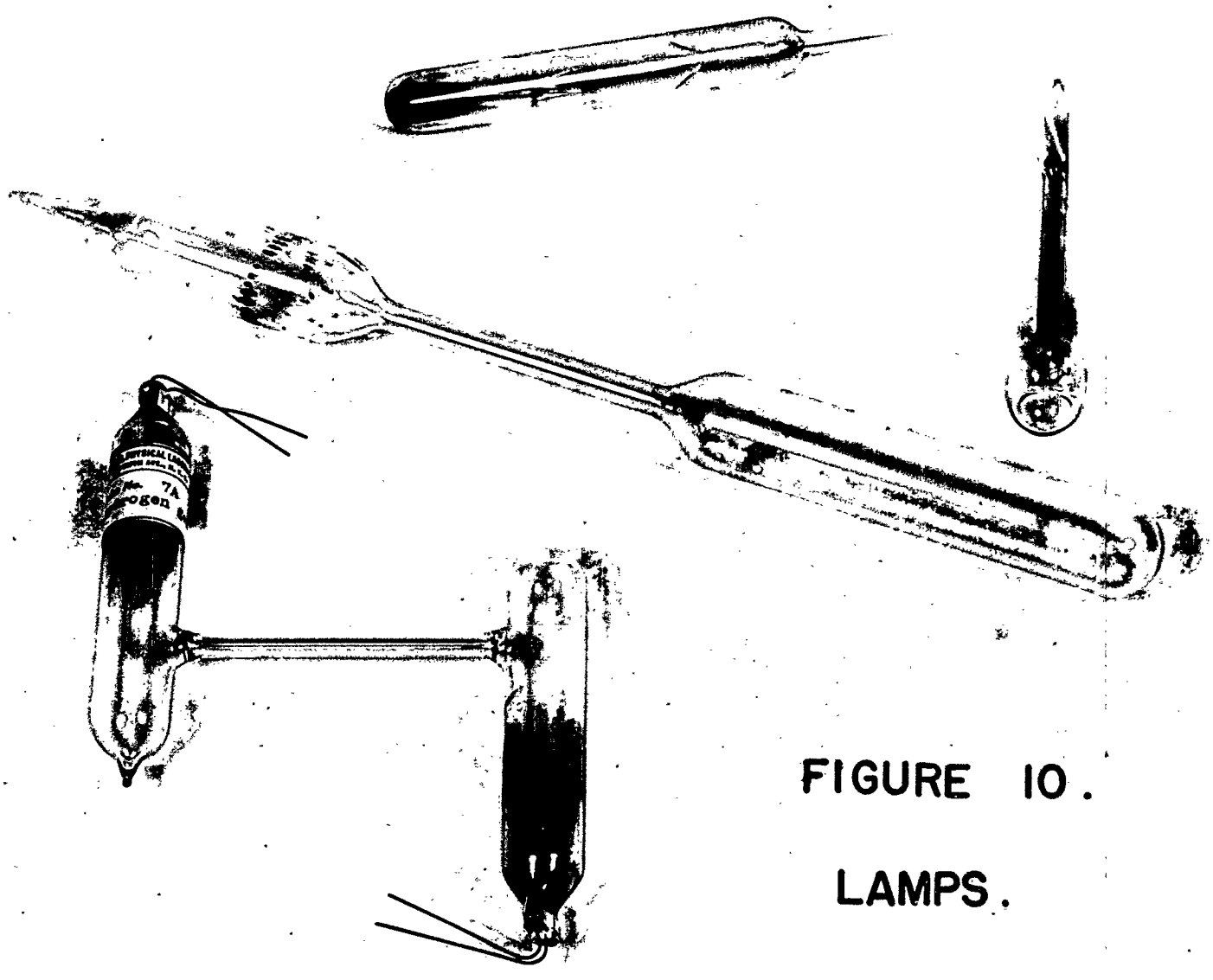

FIGURE 10.

LAMPS.

of the H-D lamps used, two electrodeless, and one with electrodes for a cold cathode Geissler type discharge.

VI. The Effect of the Fine Structure of $H\alpha$ and $H\beta$

It was apparent that there was a considerable problem in keeping the temperature of the ADP constant and uniform enough to make reproducible readings. Even when the temperature was allowed to reach equilibrium and held pretty close, there sill appeared to be some discrepancy between the angular location of the visible minima and their sharpness which was greater than the temperature effect. Therefore a search was made for other points in the theory of the device which might have been neglected.

One of these points was the natural fine structure of the $H\alpha$ line. $H\alpha$ and $D\alpha$ are separated by about 1.8 angstroms but when one investigates these lines at high resolution, it is found that each consists of seven components. The effect of this structure on the polarization H-D analyzer has been exactly calculated. In addition to this natural structure, all components are, of course, broadened in any practical source by the Doppler Effect, and possibly other source broadening effects. The elementary theory of the device considered only two monochromatic lines, H_λ and D_λ. All of these effects which broaden the line have the same general effect on the method, which, as will be shown, is to make the method insensitive below a small limiting value of the ratio D/H.

The first step was to determine from the literature the actual structure of the lines. This was done for both $H\alpha$ and $H\beta$. All that is required for this information is the reference work "Atomic Energy Levels" (Charlotte E. Moore, Circular of the NBS, #467, Vol. I, 1949).

The lines under consideration arise from the following atomic transitions:

H_α: $3s(^2S_{1/2}) \longrightarrow 2p\ (^2P^o_{3/2,1/2})$; $3d(^2D_{5/2,3/2}) \longrightarrow 3p$ and $3p\ (^2P^o_{3/2,1/2}) \longrightarrow 2s(^2S_{1/2})$

H_β: same with 4s, 4p, and 4d as initial states.

The energy levels for these transitions are indicated on Figure 11. When the selection rules are introduced, there are seven permissible transitions for each line, these being indicated on the figure by diagonal lines.

From the energy level values given in Moore's work, it was possible to derive Table I, showing the vacuum wave number (σ) and wavelength (λ), of the seven components of $H\alpha$ and the air wave number and wavelength. Table II shows the same for deuterium, Table III for tritium. Table IV lists for H and D the vacuum wave numbers measured from the H-component of lowest wave numeber, and also the relative intensities.

The conversion from air to vacuum was made by means of Edlen's[6] latest figures.

$$(n-1)\ 10^8 = 6432.8 + 2949810(146-\sigma^2)^{-1} + 25540(41-\sigma^2)^{-1} \qquad (20)$$

σ = vacuum wave numeber in μ^{-1} = $1.5233\,\mu^{-1}$

n = refractive index of dry air at 760 mm and 15° (21)

$$\lambda_{vac} = \frac{1}{\sigma_{vac}}\ ; \quad \lambda_{air} = \frac{1}{\sigma_{air}}$$

$$\lambda_{air} = \frac{1}{n}\lambda_{vac}; \quad \sigma_{air} = n\sigma_{vac}$$

For $H\alpha$: $n = 1.000,276,235$

$1/n = 0.999,723,841$

6. J. Opt. Soc. Am., 43, 339 (1953).

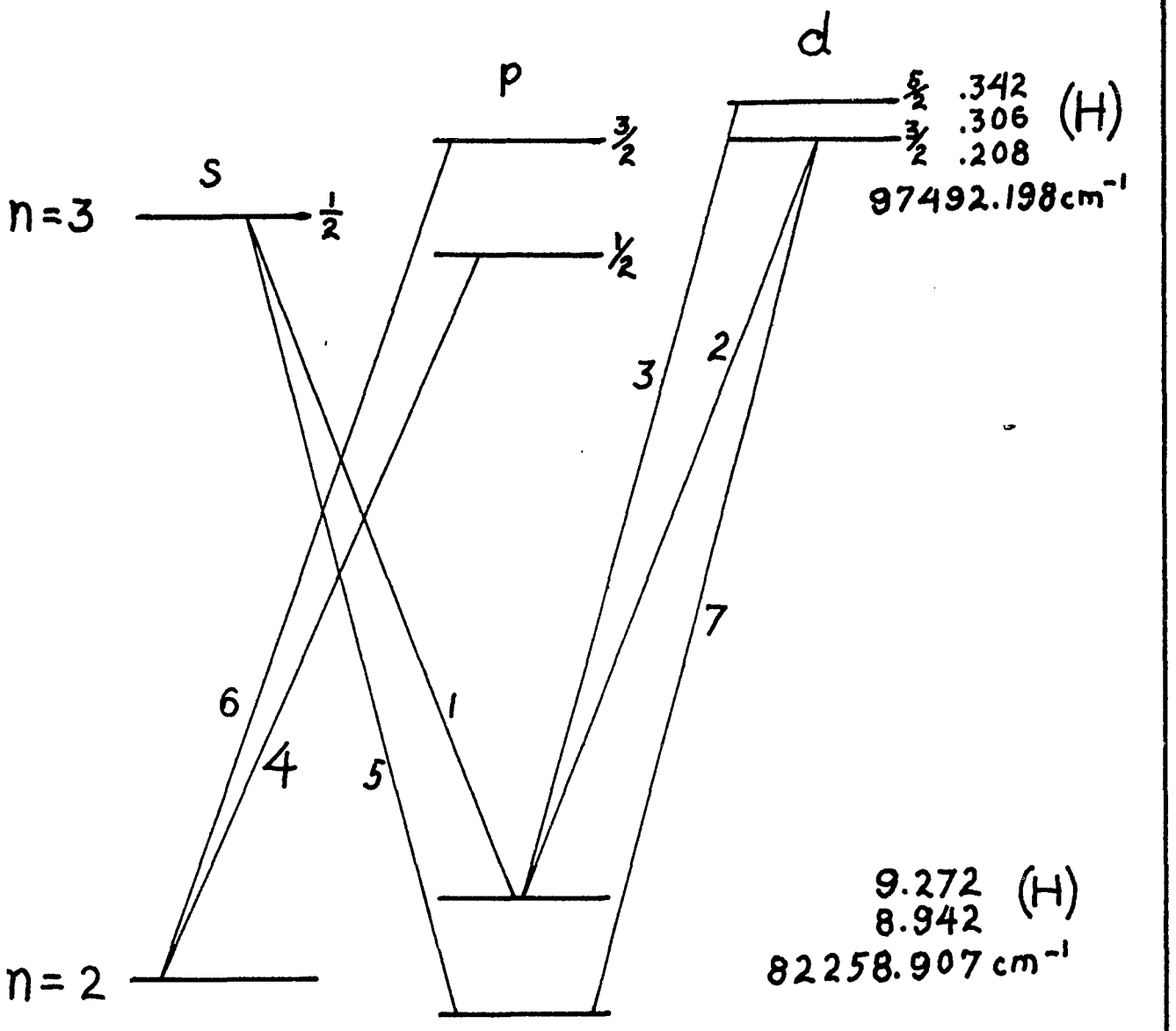

H_β has similar structure with upper level n=4 instead of n=3

Fig 11

ENERGY LEVEL DIAGRAM FOR H_α and H_β

Baird Associates, Inc.

Table I.

Hyperfine Structure of Hydrogen Alpha in
Order of Lowest Wave Number or Highest Wavelength

Transition	Vacuum Wave Number	Vacuum Wavelength	Air Wave Number	Air Wavelength
$^2S_{1/2} \rightarrow {}^2P^0_{3/2}$	15232.9359	6564.72269	15237.14377	6562.90978
$D_{3/2} \rightarrow {}^2P^0_{3/2}$	15233.0341	.68037	15237.24200	6562.86747
$^2D_{5/2} \rightarrow {}^2P^0_{3/2}$	15233.0702	.66481	15237.27811	6562.85192
$^2P^0_{1/2} \rightarrow {}^2S_{1/2}$	15233.2556	.58492	15237.46356	6562.77205
$^2S_{1/2} \rightarrow {}^2P^0_{1/2}$	15233.3010	.56535	15237.50897	6562.75249
$^2P^0_{3/2} \rightarrow {}^2S_{1/2}$	15233.3638	.53829	15237.57179	6562.72543
$^2D_{3/2} \rightarrow {}^2P^0_{1/2}$	15233.3992	.52303	15237.60720	6562.71018

Baird Associates, Inc.

Table II.

Deuterium Alpha

Transition	Vacuum Wave Number	Vacuum Wavelength	Air Wave Number	Air Wavelength
$^2S_{1/2} - {}^2P^0_{3/2}$	15237.0808	6562.93691	15241.28981	6561.12449
$^2D_{3/2} - {}^2P^0_{3/2}$	15237.1790	6562.89461	15241.38804	6561.08221
$D_{3/2} - {}^2P^0_{3/2}$	15237.2151	6562.87906	15241.42415	6561.06616
$^2P^0_{1/2} - {}^2S_{1/2}$	15237.4006	6562.79916	15241.60970	6560.98678
$^2S_{1/2} - {}^2P^0_{1/2}$	15237.4460	6562.77961	15241.65511	6560.96724
$^2P^0_{3/2} - {}^2S_{1/2}$	15237.5088	6562.75256	15241.71793	6560.94020
$^2D_{3/2} - {}^2P^0_{1/2}$	15237.5442	6562.73732	15241.75334	6560.92496

Baird Associates, Inc.

Table III.

Tritium Alpha

Transition	Vacuum Wave Number	Vacuum Wavelength	Air Wave Number	Air Wavelength
$^2S_{1/2} - {}^2P^0_{3/2}$	15238.4588	6562.34343	15242.66819	6560.53118
$^2D_{3/2} - {}^2P^0_{3/2}$	15238.5570	6562.30114	15242.76642	6560.48890
$D_{5/2} - {}^2P^0_{3/2}$	15238.5931	6562.28539	15242.80253	6560.47335
$^2P^0_{1/2} - {}^2S_{1/2}$	15238.7786	6562.20571	15242.98808	6560.39950
$S_{1/2} - {}^2P^0_{1/2}$	15238.8240	6562.18616	15243.03350	6560.37395
$^2P^0_{3/2} - {}^2S_{1/2}$	15238.8868	6562.15912	15243.09631	6560.34692
$^2D_{3/2} - {}^2P^0_{1/2}$	15238.9222	6562.14387	15243.13172	6560.33167

Baird Associates, Inc.

Table IV

Spacing Relative to H_α, and
Relative Intensities of H_α and D_α

Component	($\Delta\sigma$ vac)	($-\Delta\lambda$ vac)	Intensities
H_1	0	0	$2\sigma^4$
H_2	.0982	.04232	$20\sigma^4$
H_3	.1343	.05788	$30\sigma^4$
H_4	.2197	.13777	$1\sigma^4$
H_5	.3651	.15734	$1\sigma^4$
H_6	.4279	.18440	$2\sigma^4$
H_7	.4633	.19966	$10\sigma^4$
D_1	4.1449	1.78578	2
D_2	4.2431	1.82808	20
D_3	4.2792	1.84363	30
D_4	4.4647	1.92353	1
D_5	4.5101	1.94308	1
D_6	4.5729	1.97013	2
D_7	4.6083	1.98537	10

Intensities derived from formulae in Pauling and Goudsmit.

The relative intensities are derived from intensity rules given in Pauling and Goudsmit "Structure of Line Spectra". Although they are proportional to σ^4, this factor is essentially constant over this very narrow structure.

Table V summarizes the same information for $H\beta$, $D\beta$, and $T\beta$. For both α and β the structure is identical between H, D, and T. In addition to this "fine structure" there is the "nuclear hyperfine structure", which, however, is negligible, being a maximum of .0015 cm^{-1}.

The Doppler broadening is most readily obtained from a formula given in Tolansky's "High Resolution Spectroscopy".

$$\frac{(\Delta\sigma)_{1/2}}{\sigma_0} = 0.71 \times 10^{-6} \sqrt{T/M} \qquad (22)$$

T = absolute temperature

M = atomic mass (on scale H = 1)

$M_H = 1$; $M_D = 2$; $M_T = 3$

$\sigma_0 = 15{,}233\ cm^{-1}$ ($H\alpha$)

Table VI

T	$(\Delta\sigma)_{1/2}$-$H\alpha$	$(\Delta\lambda)_{1/2}$-$H\alpha$	
300°K	0.19 cm^{-1}	0.082 Å	For D : multiply by 1.414
500°K	0.242	0.104	
1000°K	0.342	9.147	
1500°K	0.42	0.180	

For $H\alpha$: $(\Delta\sigma)_{1/2} = 0.0108 \sqrt{T}\ cm^{-1}$

The structure of $H\alpha$ and $H\beta$ on a linear wavelength scale is shown in Figures 12 and 13. The heights are drawn proportional to the intensities and the Doppler widths are shown by horizontal lines.

Baird Associates, Inc.

Table V.

Fine Structure of $H\beta$, $D\beta$, and $T\beta$

Component	Transition	$H\beta$ Vac. Wave No.	$H\beta$ Vac. Wavelength	$H\beta$ $-\Delta\lambda$ vac	$D\beta$ $-\Delta\lambda$ vac	$T\beta$ $-\Delta\lambda$ vac
1	$^2S_{1/2} \rightarrow {}^2P^0_{3/2}$	20,564.5669	4862.73309	0	1.32267	1.76268
2	$^2D_{3/2} \rightarrow {}^2P^0_{3/2}$	.6085	.72385	.00984	1.33251	1.77252
3	$^2D_{5/2} \rightarrow {}^2P^0_{3/2}$	.6237	.71966	.01343	1.33610	1.77611
4	$^2P^0_{1/2} \rightarrow {}^2S_{1/2}$	.8926	.65607	.07702	1.39969	1.83970
5	$^2S_{1/2} \rightarrow {}^2P^0_{1/2}$	.9320	.64676	.08633	1.40900	1.84901
6	$^2P^0_{3/2} \rightarrow {}^2S_{1/2}$	.9382	.64529	.08780	1.41047	1.85048
7	$^2D_{3/2} \rightarrow {}^2P^0_{1/2}$	.9736	.63692	.09617	1.41884	1.85885

Fine Structure of $H\alpha$

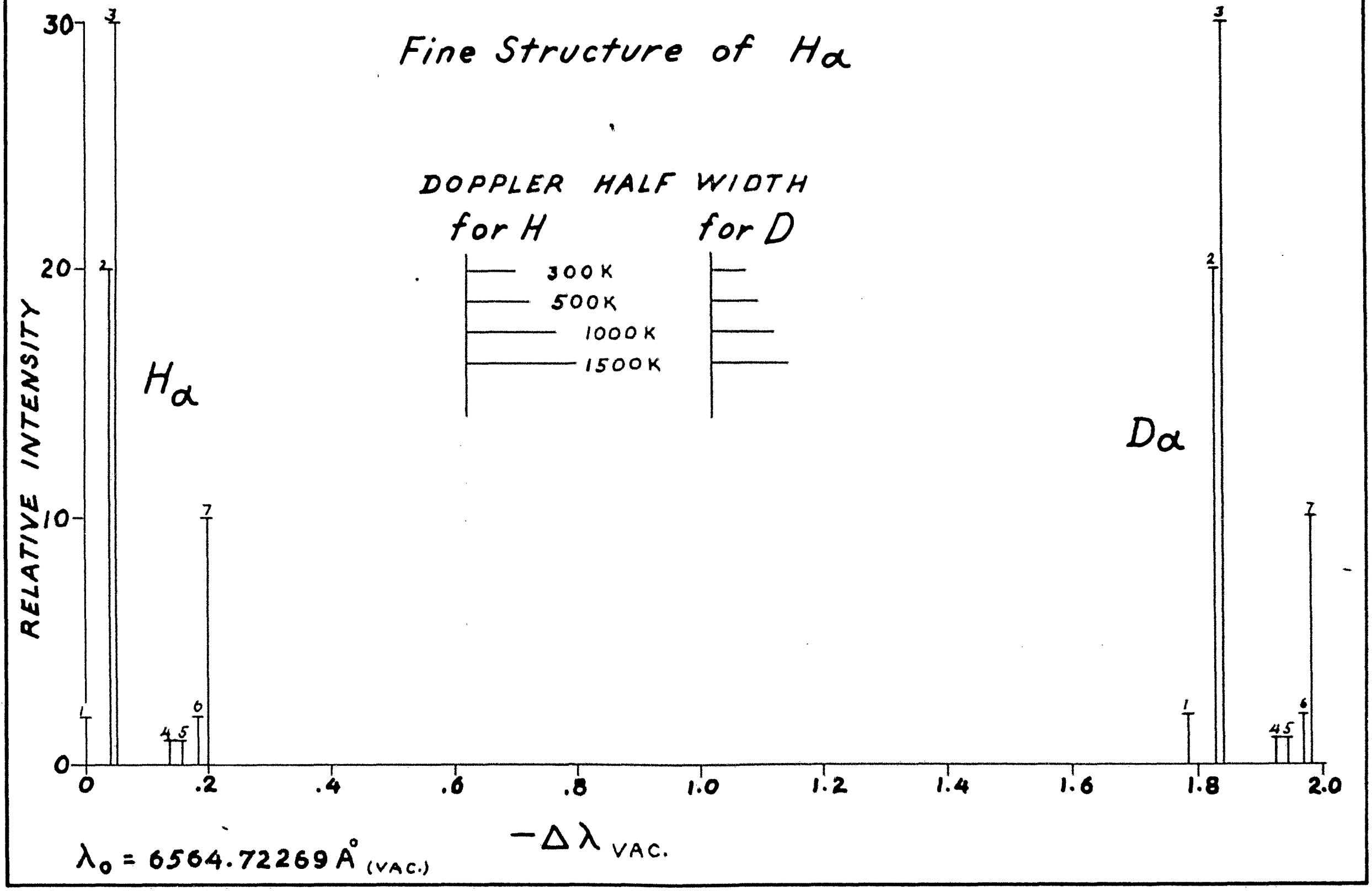

$\lambda_0 = 6564.72269\,\text{Å}_{(VAC.)}$

Fine Structure of $H\beta$

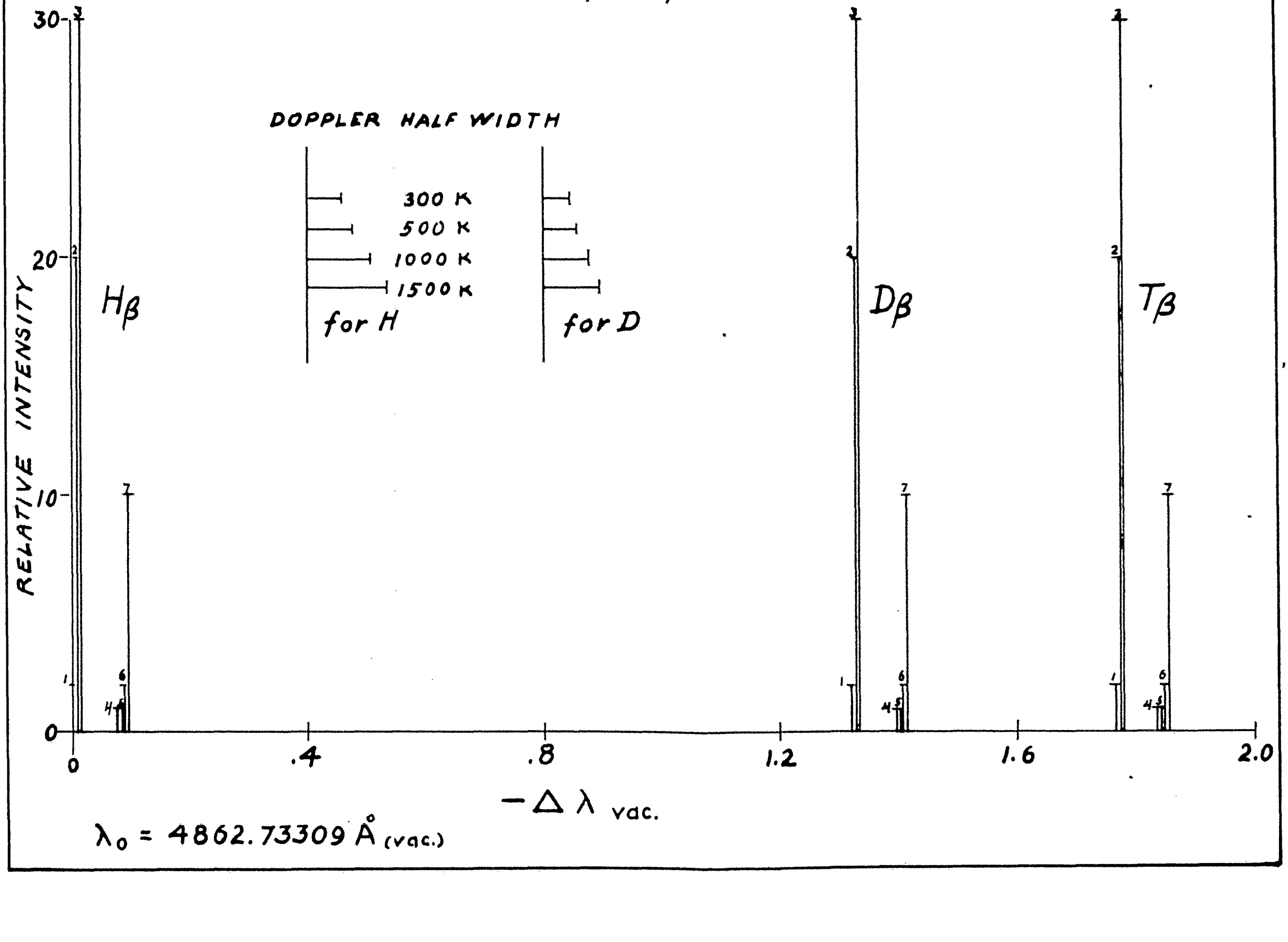

$\lambda_0 = 4862.73309$ Å (vac.)

For any reasonable Doppler half width, all seven components of these lines will not be resolved, but there will be resolved two broad lines with widths of the order of half their spacing and relative intensities 52 and 14. The center of gravity of these two groups was evaluated exactly, the stronger group containing three lines, the weaker four lines. The stronger has a center of gravity at .0497 angstroms and the weaker at .1902 angstroms, both measured from the original position of H_1, the component of the lowest wave number. The spacing from H to D is 1.7857 angstroms, so that

$$\frac{\Delta\lambda \text{ (structure)}}{\Delta\lambda \text{ (H - D)}} = \frac{.1405}{1.7858} = .0787 \qquad (23)$$

The reduction of the seven component calculations into calculations involving only two will be much easier, and, as will be evident from the type of effect produced, will not greatly alter the final result. This is particularly true because of the Doppler broadening and because four of the lines are very weak compared to the other three, and two of the strong ones are almost superposed.

In the Sage method analyzer, the retardation δ of the thick birefringent plates is chosen so that

$$\gamma_H - \gamma_D = \frac{\pi}{2} = 90 \text{ degrees} \qquad (24)$$

On the single monochromatic theory, in other words, they are polarized at right angles to each other. In the more rigorous analysis, the two components of H, denoted by A and B, will be plane polarized, but at an angle.

$$\gamma_A - \gamma_B = .0787\frac{\pi}{2} = 7.08 \text{ degrees} \qquad (25)$$

Thus with both H and D light, we have light of four monochromatic components incident on the polarization analyzer. The actual arrangement of polarizers and ADP and mica retardation plates was shown in Figure 5.

The sets ADP-M-ADP act as a single plate of retardation γ. Since γ is a function of wavelength, we have the following four values of γ and intensity at the wavelengths of the four components:

$$\begin{aligned} I_{01} &= 52H & \gamma_1 &= \epsilon_1 & \epsilon_1 &= 1.48 \text{ degrees} \\ I_{02} &= 14H & \gamma_2 &= \epsilon_2 & \epsilon_2 &= 5.60 \text{ degrees} \\ I_{03} &= 52D & \gamma_3 &= \pi/2 - \epsilon_1 & \epsilon &= \epsilon_1 + \epsilon_2 = 7.08 \text{ degrees} \\ I_{04} &= 14D & \gamma_4 &= \pi/2 + \epsilon_2 \end{aligned} \tag{26}$$

ϵ_1 and ϵ_2 have been chosen so that the center of gragity of the first two components is at zero and the last two is at 90 degrees.

Equation (14) is now replaced by

$$I = \sum_{k=0}^{4} I_{ok} \cos^2 (\sigma_k - \rho_1) \cos^2 (\gamma_k - \omega t) \tag{27}$$

for the total light intensity transmitted by all four wavelengths. This appears complex, but if we consider only the first two components

$$\frac{I_1 + I_2}{2^H} = 52 \cos^2 (\rho_1 + \epsilon_1) \cos^2 (\omega t + \epsilon_1) + 14 \cos^2 (\omega t + \epsilon_2) \cos^2 (\omega t - \epsilon_2), \tag{28}$$

which can be resolved into a D.C. component and two sinusoidal components of different amplitude and phase.

$$\frac{I_1 + I_2}{H} = 26\cos^2(\rho_1 + \epsilon_1) + 7\cos^2(\rho_1 - \epsilon_2) + 26\cos^2(\rho_1 + \epsilon_1)\cos(2\omega t + 2\epsilon_1) + 7\cos^2(\rho_1 - \epsilon_2)\cos(2\omega t - 2\epsilon_2) \quad (29)$$

We note that ρ_1 is the angle of the calibrated polarizer on the graduated circle in the measuring system. We now ask what is the amplitude of the A.C. signal generated by the spinning polarizer and consider only the contribution of I_1, and how does this amplitude vary with the position of ρ_1 of the calibrated polarizer.

$$|I_1|_{AC} = 26\cos^2(\rho_1 + \epsilon_1)$$

This is plotted in Figure 14. Similarly, for I_2 the amplitude is $7\cos^2(\rho_1 - \epsilon_2)$. These two A.C. signals are out of phase on the ρ_1 axis, that is, they reach maxima or minima for different settings of ρ_1. Further, they have a phase difference $2(\epsilon_1 + \epsilon_2)$ on the time axis, that is, they are electrically out of phase. But they may still be added with regard to phases to give a resultant whose amplitude is indicated schematically by the dotted line on Figure 14.

This simple picture can be repeated for I_3 and I_4. The two components and their resultant now are proportional to D, while $I_1 + I_2$ is proportional to H. Identical curves are obtained except displaced exactly 90 degrees on the ρ_1 axis and 180° in the electrical time axis.

Figure 15 shows how $I_1 + I_2$ are combined with $I_3 + I_4$. Since they are exactly 180° out of phase the net signal in the A. C. detector is the difference, and the four points of intersection are angles of setting for the calibrated polarizer for which a null is found. These angles of course depend on the ratio of D to H and the value of the intersection angle replaces the simple equation for the monochromatic theory:

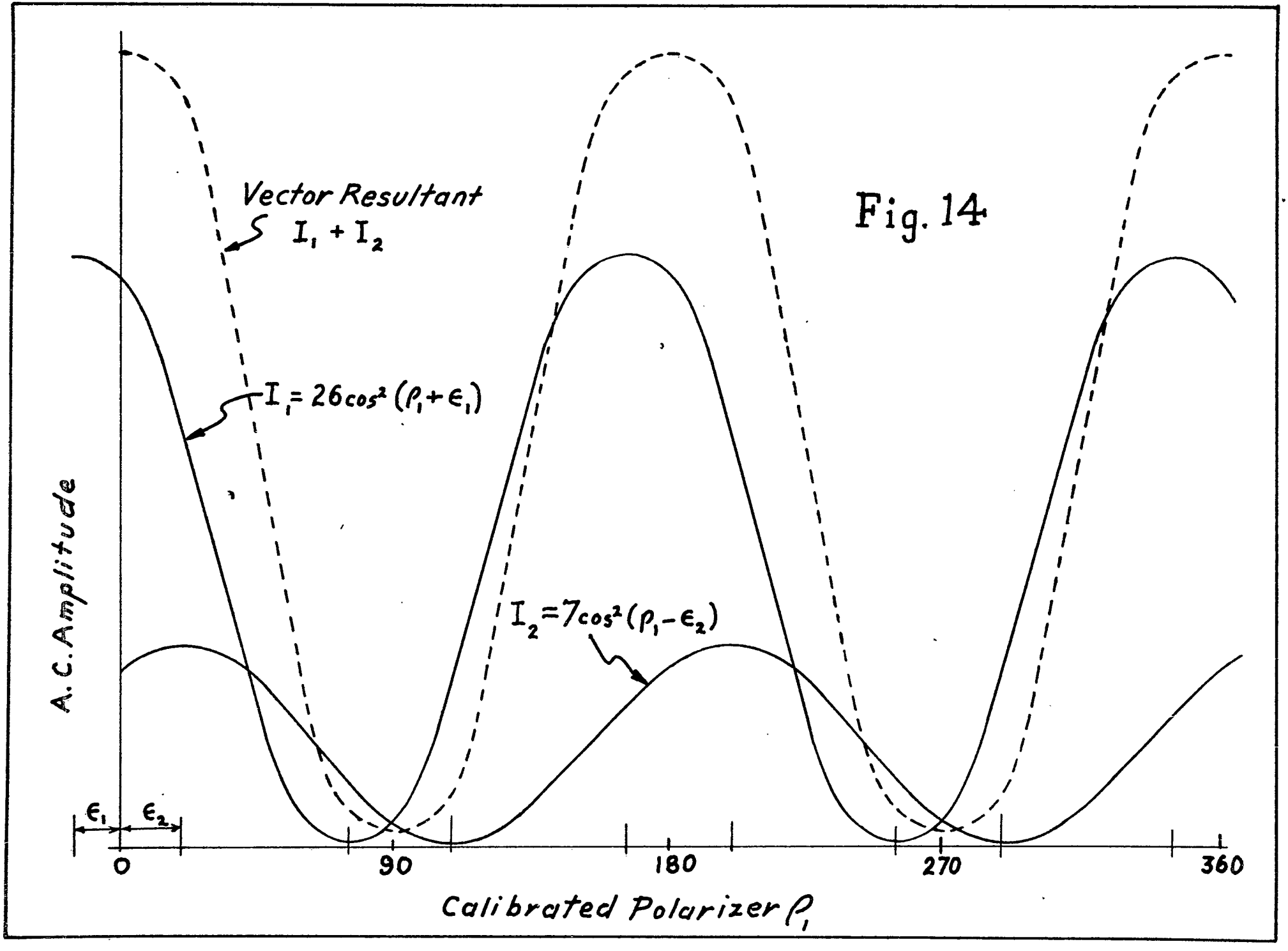
Vector Resultant
$I_1 + I_2$
$I_1 = 26\cos^2(\rho_1 + \epsilon_1)$
$I_2 = 7\cos^2(\rho_1 - \epsilon_2)$
A.C. Amplitude
ϵ_1
ϵ_2
0
90
180
270
360
Calibrated Polarizer ρ_1

Fig. 14

Fig.15

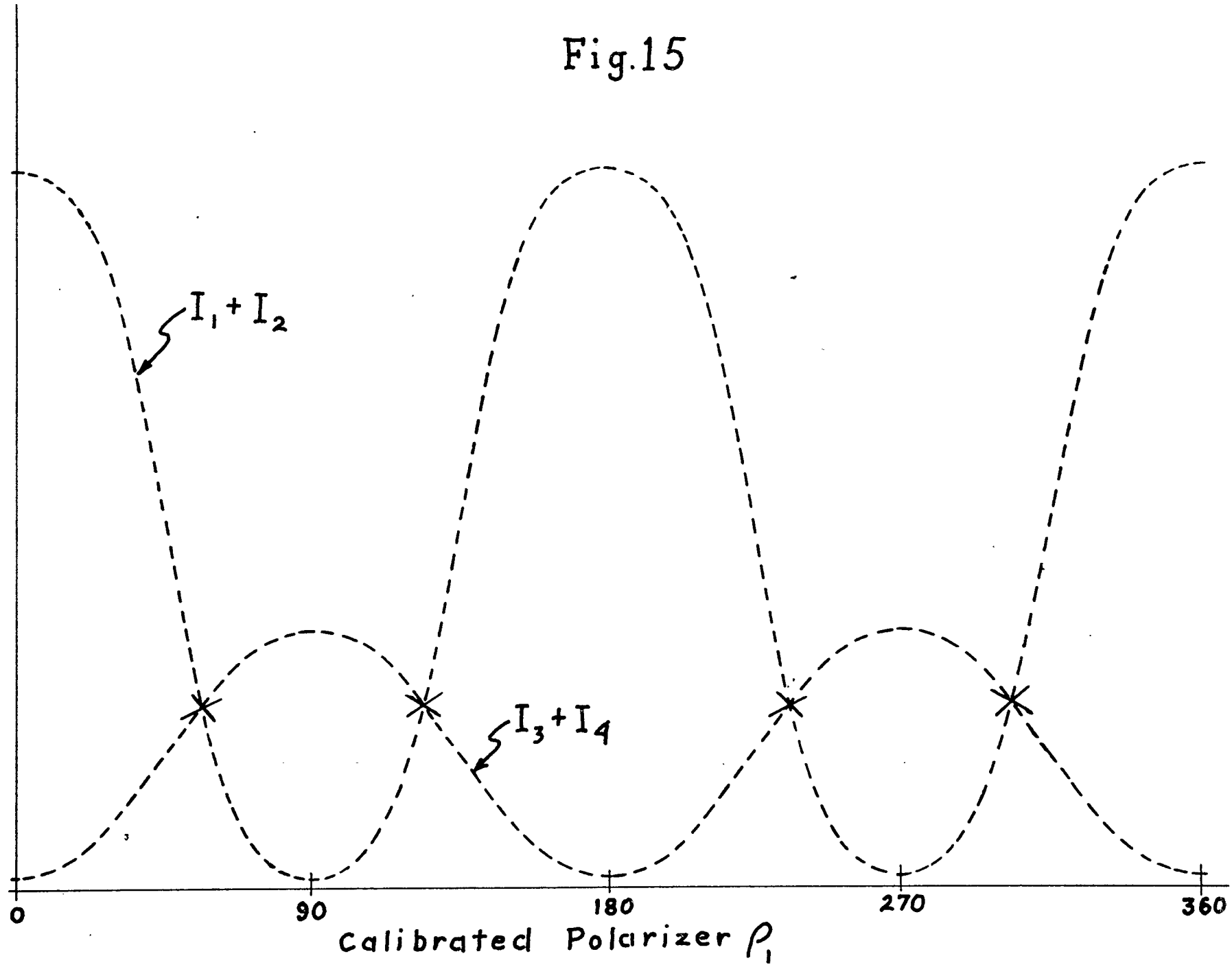
$I_1 + I_2$
$I_3 + I_4$
A. C. Amplitude
0
90
180
270
360
Calibrated Polarizer P_1

$$D/H = \tan^2 \rho_1$$

Figure 16, curve G, is an accurate enlarged plot of the final result for $I_1 + I_2$ versus ρ_1 for the stronger component of the gas mixture, assumed to be H. The extinction point on the ρ_1 polarizer scale for the two individual fine structure components is indicated. The scale is so chosen that $\rho_1 = 0$ at the center of gravity of these components. If there were no structure, $\epsilon_1 = \epsilon_2 = 0$, and the simple theory would give curve G^1. The amplitude of $I_3 + I_4$ depends on the concentration of deuterium and is plotted for D = .001, .002, .005. The intersection points are the angles for which null balance is obtained. The quantity dI_{AC}/ρ_1 which is of interest in computing the contribution of electronic noise to the error of measurement, is readily found from the slope of curve G.

The final effect of the fine structure on the calibration and on the accuracy of the method can now be discussed. As stated above, the intersection curve of $I_3 + I_4$ with G as a function D/H replaces equation (6) as the calibration curve. The most important effect is that below about D = .0025, there is no null balance at all, and further, the polarizer angle ρ_1 for minimum A.C. signal is independent of concentration. Hence D/H values less than .0025 cannot be determined at all.

On the basis of the simple monochromatic theory we have given equation (7):

$$\frac{\Delta D/H}{D/H} = 4 \csc 2\beta \, \Delta\rho_1$$

as the relative error due to an angular setting error $\Delta\rho_1$. Now for the rigorous inclusion of fine structure effects we note that curve G is the same as G^1, but displaced vertically. This means that in all respects the complete two-component theory predicts the same relative error at concentration D/H that the one-component theory would have predicted at con-

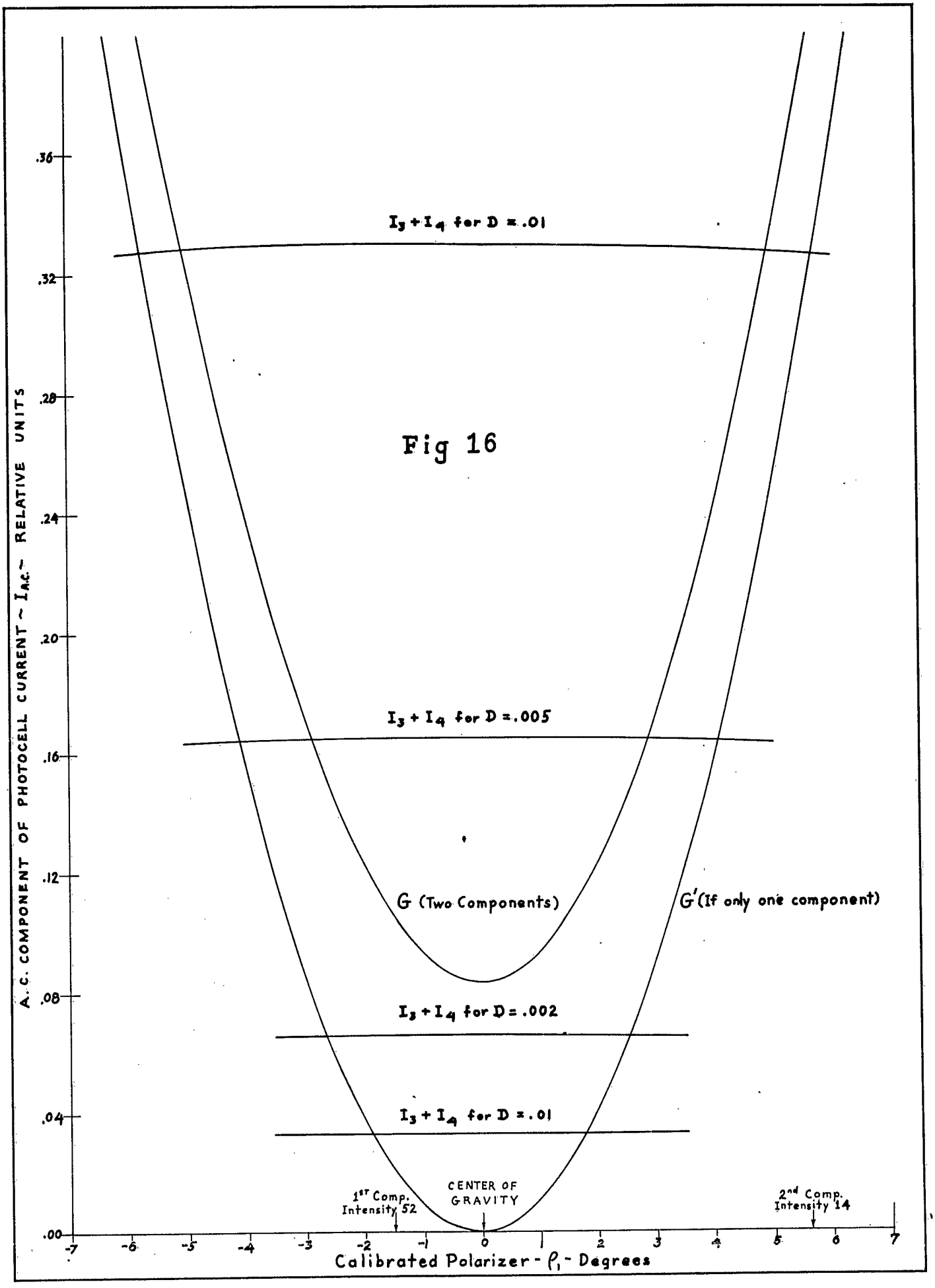
A.C. COMPONENT OF PHOTOCELL CURRENT ~ $I_{A.C.}$ ~ RELATIVE UNITS
.36
.32
.28
.24
.20
.16
.12
.08
.04
.00
$I_3 + I_4$ for D = .01
$I_3 + I_4$ for D = .005
$I_3 + I_4$ for D = .002
$I_3 + I_4$ for D = .01
G (Two Components)
G' (If only one component)
1st Comp. Intensity 52
CENTER OF GRAVITY
2nd Comp. Intensity 14
-7 -6 -5 -4 -3 -2 -1 0 1 2 3 4 5 6 7
Calibrated Polarizer - ρ_1 - Degrees

Fig 16

centration (D/H ~.0025). But we have obtained an analytical expression for the simple one-component theory, namely equation (7).

Table VII and Figure 17 shows the relative error predicted as a function of D/H and as a function of the source of error, the expected angular error in setting of the polarizer ρ. In the next section will be discussed the effect of temperature and flatness fluctuations in leading to an uncertainty of setting.

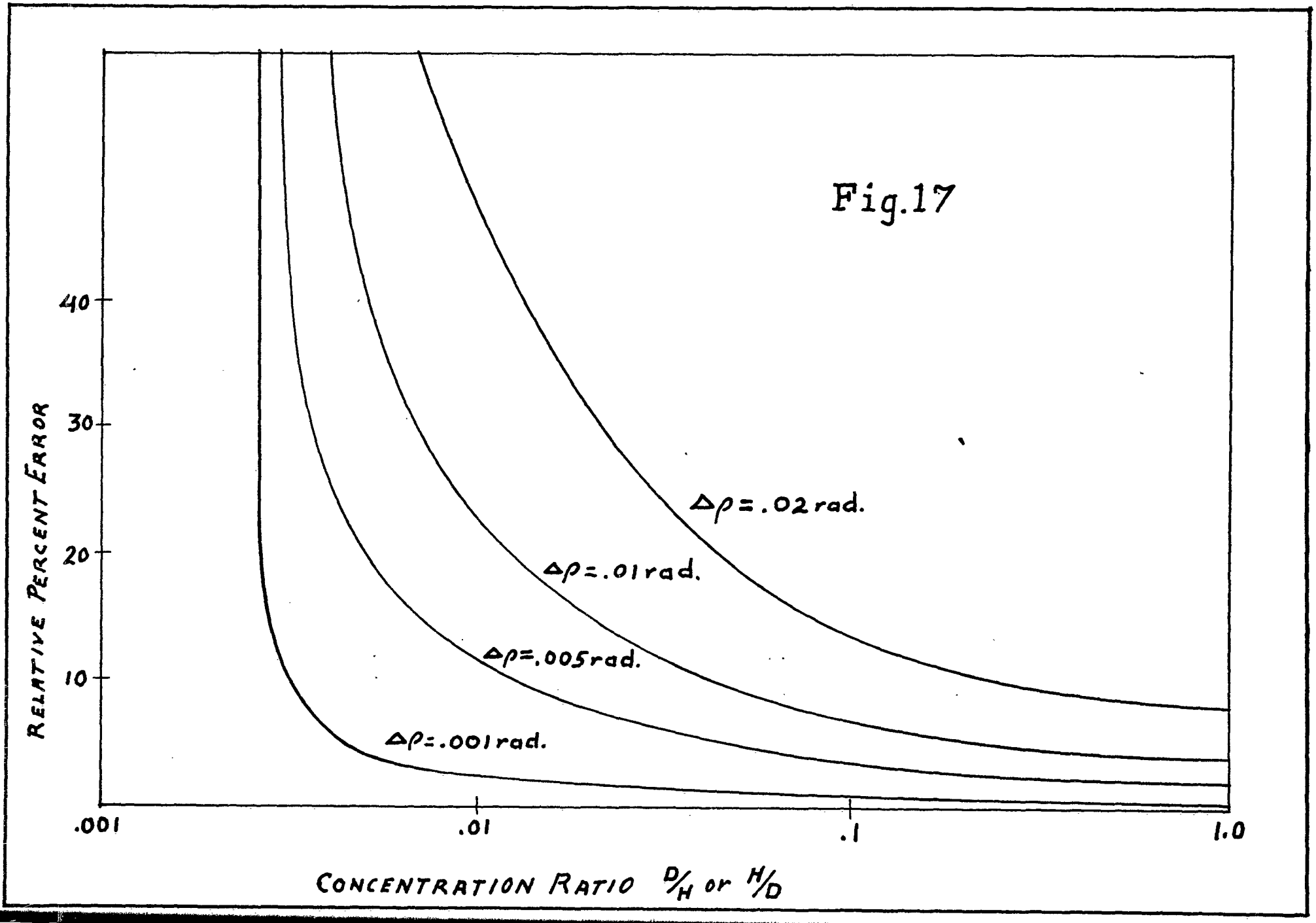
Fig.17
40
30
20
10
RELATIVE PERCENT ERROR
Δρ=.02 rad.
Δρ=.01 rad.
Δρ=.005 rad.
Δρ=.001 rad.
.001
.01
.1
1.0
CONCENTRATION RATIO D/H or H/D

Table VII

RELATIVE ERROR $\frac{\Delta(D/H)}{D/H}$ of D/H Analyzer versus D/H and Uncertainty in ANGULAR SETTING

D/H	ρ_1 simple theory	ρ_1^* corrected	4 csc $2\rho_1^*$	Relative % error for $\Delta\rho_1^*$ =			
				.001 .57	.005 .29	.01 .57	.02 rad 1.15 deg.
0-.0025	varies	0					
.005	4°4'	2°52'	10.0	4.0	20	40	80
.01	5°42'	4°55'	5.86	2.34	11.7	23	47
.02	8°4'	7°34'	3.83	1.53	7.6	15	31
.05	12°36'	12°10'	2.43	.97	4.8	9.7	19
.10	17°32'	17°20'	1.76	.70	3.5	7.0	15
.20	26°37'	26°30'	1.25	.50	2.5	5.0	10
.50	35°16'	35°16'	1.10	.44	2.2	4.4	8.8
1.00	45°	45°	1.00	.40	2.0	4.0	8.0
Column 1	2	3	4	5	6	7	8

VII. Tolerances on Flatness and Temperature Control

In the last section mathematical results have been presented for the expected relative error of measurement as a function of the uncertainty $\Delta\rho_1$ in angular setting. Now we must inquire about the magnitude of this uncertainty resulting from various sources of error in the instrument. Three of these will be principally considered:

1. The uncertainty resulting from the precision, or lack of it, in the construction of the calibrated circle, including the scale reading error.
2. The flatness of the thick retardation plates.
3. The fluctuations in temperature and the temperature gradients in the apparatus.

The calibrated circle which we used is shown in Figure 9. It originally was extracted from an old X-ray goniometer. It has a vernier scale and reads to 0.1 degrees without a magnifier and without difficulty. O. C. Rudolph and Sons make polarimeters and other precision optical apparatus containing circles accurate to about .01 degrees.

Optical polishing of crystalline plates is a highly developed art, but even with the very best "hand figuring" techniques there will still be minute fluctuations in flatness and hence thickness t across the surface of a crystalline retardation plate.

Since the retardation γ appears in terms of the form $\cos^2(\gamma-\rho_1)$, a fluctuation $\Delta\gamma$ in phase retardation will introduce an error in angular setting $\Delta\rho_1=\Delta\gamma$. By equation (15)

$$\gamma=\frac{\pi\mu t}{\lambda} \qquad (15)$$

Therefore

$$\Delta\rho \text{ (flatness)} = \Delta\gamma = \frac{\pi\mu}{\lambda}\Delta t = \frac{\pi\mu}{2}\Delta f \qquad (30)$$

It is customary to specify the flatness to which a plate can be polished in terms of the "number of interference fringes". This is a result of the use of interference fringes in the observation of the flatness of plates. If Δf is the departure in flatness in fringes

$$\lambda/2\ \Delta f = \Delta t \qquad (31)$$

The birefringence μ and the thickness t of the crystal plate will be functions of the temperature T. If the temperature fluctuates or there are gradients in the plates, errors in angular setting will be introduced which can be calculated by differentiating (15).

$$\Delta\rho \text{ (temp.)} = \Delta\gamma = \frac{\pi}{\lambda}\left(\mu\frac{dt}{dT} + t\frac{d\mu}{dT}\right)\Delta T \qquad (32)$$

The tolerance on flatness and temperature control for ADP, quartz, and calcite will now be considered. The linear expansion coefficient α is defined by

$$\frac{dt}{dT} = \alpha t_o$$

Some crystal constants for plates having a total thickness of 1840 waves of retardation are

	$\alpha \times 10^6$	μ	$d\mu/dT$	t_o (cm.)	$\frac{\Delta\rho}{\Delta T}$ (rad./deg. C)	$\frac{\Delta\rho}{\Delta f}$ (rad./fringe)
calcite	5.6	.17	1×10^{-5}	0.71	0.37	0.27
quartz	13.4	.0090	1×10^{-6}	13.4	0.72	0.014
ADP	35	.045		2.7	6.0	0.070

It appears that ADP requires the highest degree of temperature control, calcite the least. Calcite, on the other hand, requires the highest degree of flatness, quarts the least. In considering flatness,

it must be recognized that ADP cannot be polished to the same high degree of flatness that quartz or calcite can, because of the temperature expansion, brittleness, and other undesirable mechanical properties of ADP. Quartz and calcite can probably be polished to about 1/30 waves by a few excellent optical surface workers in the world, while one or two people claim to do work to about 1/75 fringe. ADP is done by Frank Cooke for Baird Associates by machine methods (which are in themselves, of course, less precise than hand figuring) to a flatness of about 1/2 fringe.

It is interesting to work the tolerance equations both ways. It would be nice, for example, if we could achieve the accuracy indicated by column 6 of Table VII ($\Delta\rho$ =.005 rad = 0.29 deg.). What flatness and temperature control would this require in ADP, calcite, and quartz?

	Flatness	Temperature Control
ADP	1/10 fringe	.0008°C
calcite	1/35 fringe	.014°C
quartz	1/3 fringe	.007°C

The other approach is to consider what seems reasonable to achieve in practice. Temperature control to .01°C. requires good equipment, but is not too hard to do. As stated above, ADP to 1/2 fringe and calcite and quartz to 1/30 fringe is about what may be expected. What then is the limiting accuracy $\Delta\rho$ to be expected for the three materials and what is the limit for each based on temperature or flatness?

	Temperature Control $\Delta\rho$	Flatness
ADP	=.060 rad.	.035 rad.
calcite	.0037	.010
quartz	.0072	.0005

There is one further difficulty with quartz, the amount which is required. About 26 centimeters of quartz will be required in the entire instrument, or four identical plates 6.5 centimeters thick. This amount of good high quality optical crystal quartz would be very difficult to find, and expensive.

The conclusion is that for the polarization interference type of H-D analyzer, calcite is the most desirable material from which to make the plates.

VIII. Conclusions and Further Work

Further consideration is being made on the tolerances in azimuth and normal incidence alignment in the several plates of the ADP interferometer. The assembly and testing of the apparatus shown in Figures 6, 7, and 8 is approaching completion. It appears that the ADP interferometer method, or better yet with calcite plates, will have usefulness for an isotope analysis situation containing only two almost monochromatic lines to be analyzed with only moderate accuracy required.

With regard to isotopic analysis with higher accuracy, work has already started on the evaluation of the air spaced Fabry-Perot interferometer as the dispersing means. Its principal limitation is the "contrast" which can be achieved. This can be greatly improved by the use of multilayer reflector techniques, which have already been applied in a few laboratories doing work with the Fabry-Perot instrument. One of the most promising ideas with respect to the use of this instrument consists of tuning through the H and D fringes by enclosing the instrument in an airtight jacket and varying the air pressure, hence its index of refraction.

Some preliminary calculations have indicated also that a polished quartz plate might be used for the spacer layer of a Fabry-Perot interferometer, and that the required tolerances are within reason. Quartz, having a definite birefringence and polishable to a prescribed thickness, and having practically no absorption, avoids almost all the difficulties reported in this report that afflicted the mica spaced Fabry-Perot.

Detailed discussions of these devices will be reserved for a later report.